

Scaling of Ablative Laser-Fusion Implosions

Claire Ellen Max, Christopher F. McKee,^(a) and W. C. Mead

Lawrence Livermore Laboratory, Livermore, California 94550

(Received 12 March 1980)

A theoretical model is presented describing the spatial structure and scaling laws of laser-driven ablative implosions. The effect of inhibited electron thermal transport is explicitly included. Simple expressions describe the ablation rate and pressure as a function of laser intensity and wavelength. The analytic results are supported by extensive comparisons with numerical hydrodynamic simulations.

PACS numbers: 52.50.Jm

Many workers have discussed scaling laws for laser-driven "exploding-pusher" targets, where heat is carried predominantly by "suprathermal" electrons.¹ In the present paper, we derive scaling laws for "ablative" targets, where heat is carried predominately by "thermal"-electron conduction.

We calculate analytically for spherical geometry in steady state the ablation rate, ablation pressure, and critical radius as functions of laser intensity, wavelength, and target size. We explicitly include effects of inhibited heat transport in a form suggested by a large body of experimental data.² Previous work on spherical laser-driven ablation was largely computational,³ and assumed that thermal transport inhibition is not important.^{4,5} The present model may be roughly applied to planar targets by setting the effective ablation radius equal to the laser-spot diameter.⁶

The ablative flow.—Classical expressions⁷ for conductivity and heat flux q are valid when the scale length for temperature variations, L_T , is much longer than the electron-ion mean free path. When gradients are so steep that L_T becomes less than a mean free path, the classical expression for q implies that the characteristic speed for heat flow is much faster than the electron thermal speed. This seems physically unreasonable, at least for electron distribution functions close to Maxwellian. A common remedy has been to postulate an upper limit on the heat flux in this regime. Frequently one expresses this "saturated" magnitude of the heat flux, q_{sat} , in terms of the electron thermal speed $v_{te} \equiv (kT_e/m_e)^{1/2}$:

$$q_{\text{sat}} = f(n_e kT_e) v_{te} \equiv 5\varphi \rho c^3. \quad (1)$$

Here n_e is the number density of electrons, f is the "flux limit" as usually defined, φ is the flux limit scaled to hydrodynamic variables, and $c = (p/\rho)^{1/2}$ is the isothermal sound speed, where p and ρ are the pressure and density. At present

the appropriate value for the flux limit f is uncertain. Free-streaming values as low as 0.1 have been suggested.⁸ Interpretation of a variety of laser-plasma interaction experiments² has been possible only when f is assumed to be approximately 0.03.

In the work below, we will take the electron heat flux to be the minimum of the classical and saturated values. We leave f as a parameter in our solutions; our only restrictions are that f be constant in space, and, for the analytic work, that f be ≤ 0.4 for DT.

A typical temperature profile $T(r)$ for a laser fusion target has a high temperature at the critical radius, and a low temperature at the ablation surface. As a result, one can show that conduction is typically classical near the cold pellet surface R_a whereas it may be saturated near the critical surface.

The overall flow is obtained by solving separately in the classical and saturated regimes, and then matching the solutions at the point where the classical and saturated heat flows are equal. Details of the derivation not presented here are discussed in Refs. 3 and 8. The equations to be solved are mass conservation, the equation of motion for the gas, and the energy equation:

$$\dot{m} \equiv 4\pi r^2 \rho v = \text{const}, \quad (2)$$

$$\rho v \, dv/dr = -dp/dr, \quad p = \rho c^2, \quad (3)$$

$$r^{-2} (d/dr) r^2 \{ \rho v (v^2/2 + 5c^2/2) \} + \vec{q} \cdot \hat{r} = I\delta(r - r_c). \quad (4)$$

We assume a quasisteady state, and discuss below the validity of this assumption. Here v is the radial flow velocity, and I the absorbed laser intensity at the critical surface. For this work we assume the electron and ion temperatures to be equal; extension to separate values of T_e and T_i is straightforward.⁸ The pressure is given by $p = n_e kT_e + n_i kT_i \equiv \rho kT/\mu$. The mean mass per par-

ticle is $\mu \equiv Am_p/(Z+1)$, where the ion mass and charge are Am_p and Ze . The critical surface for a laser of frequency ω lies at the radius r_c , where the electron density is $n_c \equiv m_e \omega^2/(4\pi e^2)$. It is assumed that the laser deposits its energy at r_c . We are thus neglecting absorption in the underdense plasma ($r > r_c$). We also assume that the laser-light pressure is negligible.

Inside the pellet surface Eq. (4) may be integrated to obtain

$$\frac{5}{2} \dot{m} c^2 (1 + \frac{1}{5} M^2) + 4\pi r^2 \vec{q} \cdot \hat{r} = A = \text{const}, \quad (5)$$

where $\dot{m} = 4\pi r^2 \rho v$ is the mass loss rate and $M = v/c$ is the isothermal Mach number. The constant of integration A is the difference between the outward enthalpy flux and the inward conductive heat flux. For subsonic ablation of an unpreheated pellet, both terms are very small at the pellet surface so that $A = 0$. Reference 3 shows that this approximation is an excellent one in the regime in question.

In the *classical* region close to the pellet surface, Eq. (5) can be solved analytically in the limit $M^2/5 \ll 1$:

$$T/T_c = (\dot{m}/\dot{m}_c)^{2/5} (1 - R_a/r)^{2/5}, \quad (6)$$

where $\dot{m}_c \equiv 16\pi \mu \kappa(r_c) R_a / 25k$ is the ablation rate that would obtain if the classical region extended out to the critical surface. In fact, the heat flux reaches the saturated value in Eq. (1) at some radius $r_s < r_c$.

In the *saturated* region ($r_s < r < r_c$) the energy equation is simply $M_s(1 + M_s^2/5) = 2\varphi$, where φ is

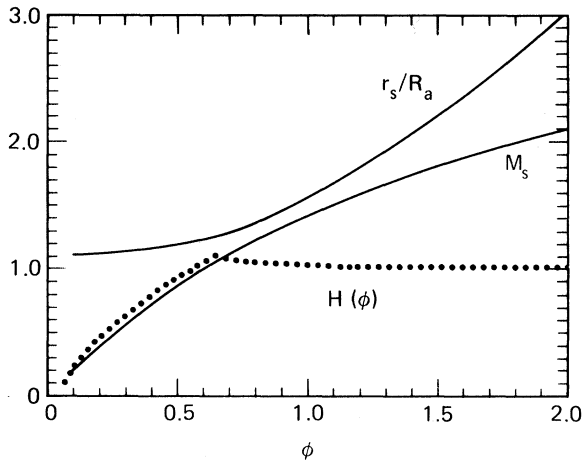


FIG. 1. Dependence on flux limit of M_s , the Mach number in the saturated region; r_s , the radius where the saturated region begins; and the function $H(\varphi)$ defined in Eq. (10).

the renormalized flux limit defined by $q_{\text{sat}} \equiv 5\varphi \rho c^3$. We conclude that the Mach number in the saturated zone, M_s , is constant and depends only on the flux limit φ (see Fig. 1). The flow is supersonic in the saturated zone for $\varphi \gtrsim 0.6$. The momentum and continuity equations yield

$$\begin{aligned} T &= T_c (r/r_c)^{4/(1+M_s^2)}, \\ \rho &= \rho_1 (r/r_c)^{(2+M_s^2)/(1+M_s^2)} \end{aligned} \quad (7)$$

in the saturated region, where $\rho_1 \equiv \rho(r_c - \delta r)$.

The dynamics in the classical zone are discussed in Ref. 8. The Mach number increases monotonically, reaching M_s at the point r_s ; hence the assumption $M^2 \ll 5$ made in deriving Eq. (6) is approximately valid for $\varphi \lesssim 1$ ($M^2 \lesssim 2$). For larger values of φ , the energy and momentum equations do not decouple, and they must be solved simultaneously.⁴ There is a family of subsonic solutions ($M_s < 1$, $\varphi \lesssim 0.6$) and a unique transsonic solution.

The ablation rate \dot{m} can be obtained if the above equations are supplemented by the jump conditions at the critical surface. Mass, momentum, and energy conservation imply

$$[\rho v] = 0, \quad [\rho v^2 + \rho c^2] = 0, \quad (8)$$

$$(\dot{m}/4\pi r_c^2) [\frac{1}{2} v^2 + \frac{5}{2} c^2] + [q] = I, \quad (9)$$

where $[y] \equiv y(r_c + \delta r) - y(r_c - \delta r)$ for any variable y . Since the temperature is a maximum at r_c where the laser energy is deposited, the jump in the heat flux at r_c is $[q] = 5\varphi(\rho_1 + \rho_2)c_c^3$, provided the heat flux is saturated on both sides of critical (the case of classical heat flow for $r > r_c$ is analyzed in Ref. 3). Here $\rho_{1,2} \equiv \rho(r_c \pm \delta r)$, $c_c \equiv c(r_c)$, and T is assumed continuous. Equation (9) then gives

$$kT(r_c) = \mu (I/10\varphi\rho_c)^{2/3} H^{2/3}(\varphi), \quad (10)$$

where the function H is derived in Ref. 3 and is plotted in Fig. 1.

Scaling laws.—We have now described solutions in the classical zone near the ablation surface, and in the flux-limited region inside the critical surface. Next the global structure of the flow and its macroscopic properties are found by matching these separate regions together.

The classical and saturated solutions within r_c must match onto each other at the point r_s where the classical and saturated heat flows are first equal.^{3,8} For subsonic flow ($M_s < 1$, $\varphi \lesssim 0.6$) one finds $r_s = R_a(11 + M_s^2)/10$. For $\varphi > 0.6$, r_s is that radius where the transsonic solution for $M(r)$ passes through M_s : $M(r_s) = M_s$. The resulting

function $r_s(\varphi)/R_a$ is plotted in Fig. 1.

For simplicity we now specialize to the flux-limit value $\varphi = 0.3$, $f \approx 0.03$, which seems most widely supported by 1.06- μm experiments. We also assume $A \approx 2Z \gg 1$. Then the ablation rate \dot{m} and pressure p_a are given by³

$$\dot{m} \approx 2.3 \times 10^4 \left[\frac{I_{14}^{0.48}}{\lambda_{\mu\text{m}}^{0.82}} \left(\frac{R_a}{0.1 \text{ cm}} \right)^{1.89} \right] \text{ g/sec, (11)}$$

$$p_a \approx 7.2 \left[\frac{I_{14}^{0.57}}{\lambda_{\mu\text{m}}^{0.99}} \left(\frac{ZR_a}{0.1 \text{ cm}} \right)^{0.07} \right] \text{ Mbar, (12)}$$

where I_{14} is the absorbed laser intensity at R_a in units of 10^{14} W/cm^2 , $\lambda_{\mu\text{m}}$ is the laser wavelength in microns, Z is the ionic charge, and R_a the pellet's ablation radius. Similarly, the radius and temperature of the critical-density surface are

$$r_c = 1.6 R_a I_{14}^{0.11} \lambda_{\mu\text{m}}^{0.38} \left(\frac{0.1 \text{ cm}}{ZR_a} \right)^{0.08}, \quad (13)$$

$$T_c = 1.7 I_{14}^{0.52} \lambda_{\mu\text{m}}^{0.83} \left(\frac{ZR_a}{0.1 \text{ cm}} \right)^{0.11} \text{ keV. (14)}$$

Figure 2 illustrates these scaling relations, and compares them with results³ of the hydrodynamics computer code LASNEX.⁹ Figure 3 illustrates typical density and temperature profiles from the present theory, for laser power $P_L = 78.5 \text{ TW}$. These compare quite well with LASNEX calculations.

These results of our model show that shorter-wavelength lasers should produce higher ablation rates and pressures for the same laser intensity and target parameters. Alternatively, to produce a given ablation pressure, i.e., a given target implosion, a higher-intensity laser is required at longer wavelengths. From Eq. (12) with p_a , Z , and R_a fixed, the scaling $I \propto \lambda_L^{1.7}$. Collective effects of hot electron production and stimulated scattering not included in our model would tend to exacerbate this already strong wavelength scaling.

We end with a brief discussion of limitations on the validity of our theory, due to various assumptions we have made. These limits are considered in detail in Ref. 3. Neglect of inverse bremsstrahlung absorption in the underdense plasma places a lower bound on the laser power or a lower bound on the laser wavelength. An upper limit on the allowable laser power arises from our assumption that an electron heated at the critical surface will not be able to penetrate to the classical zone without suffering a collision. Our neglect of hot electrons is valid when the fraction

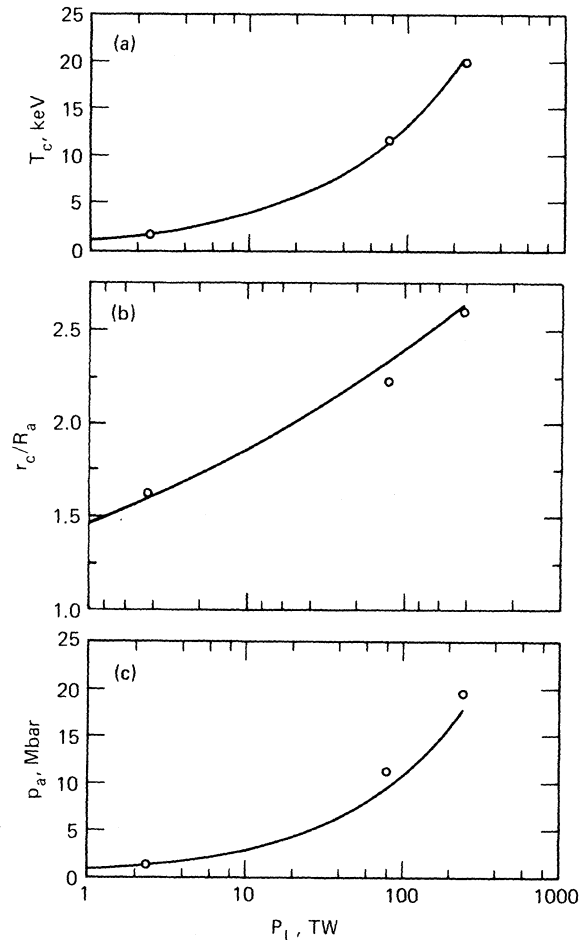


FIG. 2. Parameter study showing (a) temperature at critical T_c , (b) critical radius r_c , and (c) ablation pressure p_a as a function of absorbed laser power P_L in terawatts (1 TW = 10^{12} W). Other parameters are $\lambda_L = 2.65 \mu\text{m}$, $R_a = 0.1 \text{ cm}$, $\varphi = 0.3$, $Z = 6$, $A = 12$. Solid line is theoretical prediction. Points are results of computer hydrodynamics calculations described in Ref. 3.

of suprathermals is $\lesssim 10\%$ at the critical surface, as is seen in long-pulse or short-wavelength experiments. The steady-flow hypothesis means that our theory is valid only when the laser parameters vary slowly compared to the time it takes a fluid element to travel from the ablation surface to the critical surface. Within these limitations, extensive comparisons with computational hydrodynamics calculations³ have shown the present theory to be accurate to better than 10%, as illustrated in Fig. 2.

We thank J. H. Nuckolls, J. D. Lindl, and J. Arons for illuminating discussions. This work

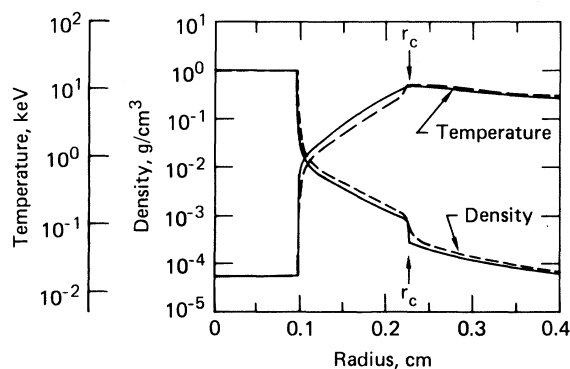


FIG. 3. Spatial profiles of density and temperature, for laser power $P_L = 78.5$ TW and other parameters as in Fig. 2. Solid lines show theoretical predictions; dashed lines are numerical results using the hydrodynamics code LASNEX. The two agree quite well.

was performed under the auspices of the U. S. Department of Energy under Contract No. W-7405-eng-48.

^(a)Permanent address: Physics Department, University of California, Berkeley, Cal. 94720.

¹M. D. Rosen and J. H. Nuckolls, *Phys. Fluids* **22**, 1393 (1979); E. K. Storm, J. T. Larsen, J. H. Nuckolls, H. G. Ahlstrom, and K. R. Manes, University of Cal-

ifornia Report No. UCRL-79788, 1977 (unpublished); D. V. Giovanelli and C. W. Cranfill, University of California Report No. LA-7218-MS, 1978 (unpublished); B. Ahlborn and M. Key, Rutherford Laboratory Report No. RL-79033, 1979 (to be published).

²R. C. Malone, R. L. McCrory, and R. L. Morse, *Phys. Rev. Lett.* **34**, 721 (1975); R. A. Haas, W. C. Mead, W. L. Kruer, D. W. Phillion, H. N. Kornblum, J. D. Lindl, D. MacQuigg, V. C. Rupert, and K. G. Tirsell, *Phys. Fluids* **20**, 322 (1977); B. Yaakobi and T. Bristow, *Phys. Rev. Lett.* **38**, 350 (1977); M. D. Rosen, D. W. Phillion, V. C. Rupert, W. C. Mead, W. L. Kruer, J. J. Thomson, H. N. Kornblum, V. W. Slivinsky, G. J. Caporaso, M. J. Boyle, and K. G. Tirsell, *Phys. Fluids* **22**, 2020 (1979).

³C. E. Max, C. F. McKee, and W. C. Mead, University of California Report No. UCRL-83542 (to be published).

⁴S. J. Gitomer, R. L. Morse, and B. S. Newberger, *Phys. Fluids* **20**, 234 (1977); L. Montierth and R. L. Morse, to be published.

⁵Yu. V. Afanas'ev, E. G. Gamalii, O. N. Krokhin, and V. B. Rozanov, *Zh. Eksp. Teor. Fiz.* **71**, 594 (1976) [*Sov. Phys. JETP* **44**, 311 (1977)].

⁶R. McCrory, R. Morse, and C. Verdon, *Bull. Am. Phys. Soc.* **23**, 787 (1978).

⁷L. Spitzer, Jr., *Physics of Fully Ionized Gases* (Wiley-Interscience, New York, 1967), Chap. 5.

⁸L. L. Cowie and C. F. McKee, *Astrophys. J.* **211**, 135 (1977).

⁹G. B. Zimmerman and W. L. Kruer, *Comments Plasma Phys. Controlled Fusion* **2**, 85 (1975); G. B. Zimmerman, University of California Report No. UCRL-74811, 1973 (unpublished).

Interface between Superfluid and Solid ^4He

J. Landau, S. G. Lipson, L. M. Määttänen, L. S. Balfour, and D. O. Edwards^(a)

Department of Physics, Technion-Israel Institute of Technology, Haifa, Israel

(Received 24 March 1980)

With an optical technique it is found that the equilibrium interface between superfluid and hcp ^4He is partially faceted, showing that at least some of it is atomically smooth. This conclusion is also consistent with the behavior of the crystal during melting and growth. The surface tension α_{LS} on the rounded part of the interface is found to be independent of temperature.

PACS numbers: 67.40.Kh, 67.80.Gb, 68.45.-v

Andreev and Parshin (AP) have discussed¹ the theory of the ^4He crystal-superfluid interface. They conjecture that the interface is atomically rough, even at $T = 0$, due to nonlocalized, zero-point quantum-mechanical defects. Since the surface is rough they predict the interfacial surface tension α_{LS} to be a smooth function of the surface orientation with respect to the crystal axes. It follows that the equilibrium shape of the crystal

should be rounded, with no facets, in agreement with several experimental observations.² AP also predicted the existence of "melting-freezing" capillary waves on the interface. These have recently been discovered by Keshishev, Parshin, and Babkin.³

This Letter reports results of a study with use of an optical-holographic technique.⁴ In general, our observations confirm the fluidlike behavior